STRUCTURE COMPATIBILITY OF GRAPHITE AND PHASES FORMED FROM ALUMINUM OR MAGNESIUM PHYLLOSILICATES

[1]Jonáš MOLEK, [1]Jonáš TOKARSKÝ

[1]*VSB - Technical University of Ostrava, Ostrava, Czech Republic, EU, jonas.molek.st@vsb.cz, jonas.tokarsky@vsb.cz*

https://doi.org/10.37904/nanocon.2025.5031

Abstract

Calcination of phyllosilicate/organics nanocomposites in inert atmosphere leads to in situ formation of graphitic carbon layers on silicate phases. Electrically conductive material (ceramics) is thus obtained. Despite an intensive research in this area, attention has not yet been paid to carbon/silicate interfaces in these systems. This study is focused on structure compatibility of graphitic carbon and the most abundant phases formed by transformation of aluminum phyllosilicates or magnesium phyllosilicates, i.e. cristobalite, mullite, forsterite, and protoenstatite. The aim is to find whether the phases can or cannot have a significant influence on the graphitic structure formation, and if the type of phyllosilicate (aluminum or magnesium) must be taken into account. Structure compatibility is determined by original method calculating the overlaps of atomic pairs carbon/another element. Carbon atoms lie in graphite(001) plane, atoms of another element lie in the given phase(hkl) plane. Different crystallographic planes of phases formed from the original phyllosilicates exhibit various structure compatibility with the graphite. The average number of overlaps of individual graphite(001)/phase(hkl) systems revealed the highest structure compatibility for mullite (M) followed by forsterite (F), protoenstatite (P) and cristobalite (C), namely M(102) > F(001) > P(100) > C(100). This sequence suggests that aluminum phyllosilicates, from which M is formed, could be a more suitable input component compared to magnesium phyllosilicates, from which F and P are formed. The lower number of overlaps for C compared to other phases indicates its small contribution to the overall structure compatibility.

Keywords: Structure compatibility, graphitic carbon, silicate, aluminosilicate, magnesium silicate

1. INTRODUCTION

Graphitic carbon can be prepared by pyrolysis of macromolecules/phyllosilicate nanocomposites [1-17]. The phyllosilicate component is transformed into cristobalite and, depending on the type of phyllosilicate, also into mullite (Al-rich) or forsterite and/or protoenstatite (Mg-rich) [5,9,15]. While possible applications of these pyrolyzed nanocomposites have been investigated (electrical conductivity [6,7,12,13], hydrogen storage [9], wastewater treatment [10] or coatings absorbing solar radiation [11] to name a few), the study of the structure is usually focused only on the determination of the formed graphitic carbon. Moreover, the carbon is often liberated from the pyrolyzed nanocomposite by etching [1-5,10,17]. Little is known about the mutual interactions of the graphite with different crystallographic planes of the inorganic phases in these pyrolyzed nanocomposites. The question of the interaction remains at the edge of interest in the field of research on these nanocomposites. Our previous work revealed that the determination of mutual interaction of two phases from optimized molecular model can be successfully replaced by a simple method quantifying the interaction by the number of overlapping atoms of two crystallographic planes, each of which belongs to one of the phases [18]. The higher the number of overlaps, the more the given crystallographic planes are structurally compatible [18]. In this study, the method was used to determine the structure compatibility of the basal graphite(001) plane and various crystallographic planes of cristobalite, mullite, protoenstatite, and forsterite. Knowledge of

the compatibility of in situ prepared graphitic carbon and silicate phases can be useful for the preparation of electrically conductive ceramics from these pyrolyzed nanocomposites.

2. MATERIALS AND METHODS

2.1 Structure compatibility

Determining the structure compatibility of two phases is based on a purely geometric point of view [18]. Two crystallographic planes, each from one phase, are placed in the same geometric plane so that one atom of each plane lies at the origin of the coordinates. In this study, one crystallographic plane was always (001) plane of graphite (G), the other crystallographic plane was (hkl) plane of cristobalite (C), mullite (M), forsterite (F) and protoenstatite (P). The calculation is performed using an algorithm that quantifies the amount of overlaps of carbon atoms from G(001) plane with another elements from C(hkl), M(hkl), F(hkl) or P(hkl) planes. An overlap is considered a state when the centers of atoms of such a pair are at a mutual distance equal to or less than 1 Å. This value is the average of the covalent radii of considered elements, i.e. 1.21, 1.41, 0.66, 1.11, 0.73 Å for Al, Mg, O, Si, C, respectively [19]. As the area of both crystallographic planes increases, the number of overlaps increases as well, while the number of overlaps relative to the unit area converges. Our earlier investigations showed the area of 100×100 Å to be optimal [18]. The two (hkl) planes are not static during the process of calculating structure compatibility. The in-plane rotation of one plane with respect to the other has a fundamental effect on the number of overlaps. Therefore, the structure compatibility is calculated as an average number of overlaps reflecting the individual values of the number of overlaps at all mutual in-plane orientations. Our earlier investigations showed the rotation step of 1° to be optimal [18]. Each input data file describing the distribution of atoms in a given (hkl) plane consists of at least one line with six Cartesian coordinates: position of the center of given atom (x, y), direction (dx1, dy1) of copying the atom to create a row, and direction (dx2, dy2) of copying an entire row to create the plane. In the case of more complex patterns, the input data may consist of more than one line of coordinates. Due to the periodicity of the atomic arrangement, these coordinates allow creating a given (hkl) plane of arbitrary dimensions.

2.2 Input data

Unit cells of G (a = b = 2.456 Å, c = 6.696 Å, α = β = 90°, γ = 120°), C (a = b = 4.978 Å, c = 6.948 Å, α = β = γ = 90°), M (a = 7.663 Å, b = 5.767 Å, c = 7.492 Å, α = β = γ = 90°), F (a = 4.754 Å, b = 10.197 Å, c = 5.981 Å, α = β = γ = 90°), and P (a = 9.250 Å, b = 8.780 Å, c = 5.320 Å, α = β = γ = 90°) [20,21] were cut along (hkl) planes selected according to the flatness and density of occupation of atoms [18]. These (hkl) planes served as a source of input data used for the structure compatibility calculation. Input data of the same (hkl) plane but with different atoms at the origin of coordinates are distinguished by I and II (see an example in **Figure 1a**).

Many (hkl) planes are not completely planar and contain atoms slightly deviated from the central plane. Strict requirement of selecting only atoms lying in a geometrically perfect plane would mean the creation of input data with an unrealistically low density of atoms. Therefore, atoms distant in the perpendicular direction from the central plane by no more than the covalent atomic radius (1.21, 1.41, 0.66, 1.11 Å for Al, Mg, O, Si, respectively [19]) were included in the input data. The (hkl) planes gradually filled with such atoms are marked with letters a,b,c (see an example in **Figure 1b**). In a case of the (hkl) planes without perfect planarity, deviations from the planarity were calculated as the perpendicular distances of atoms from the central geometric plane defined by three other atoms of a given (hkl) plane. Different arrangements of atoms in parallel (hkl) planes of the same phase, whose mutual distance (perpendicular to the plane) is greater than the covalent radius of the atoms, are marked with numbers 1-3 (see an example in **Figure 1c**). For completeness, the elements present are also listed in the designation of each (hkl) plane. Unit cells and input data are provided in Supplementary material [22].

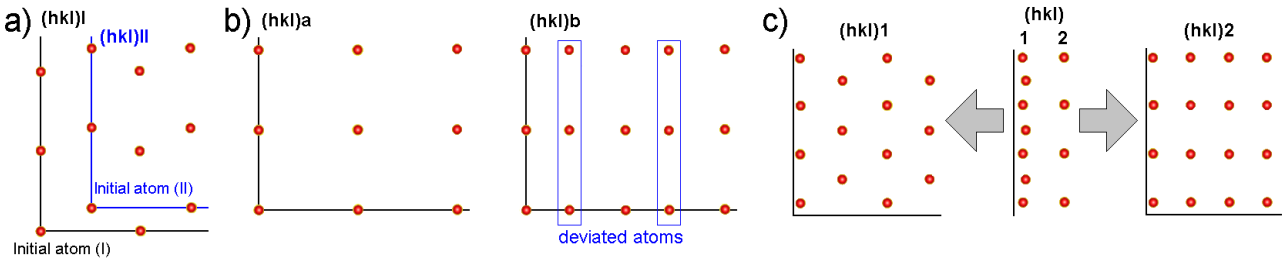

Figure 1 a) Top view of the same (hkl) plane with different atoms at the origin of coordinates (initial atoms); b) Top view of the (hkl) plane gradually filled with atoms deviated from the planarity; c) Side view of two parallel (hkl) planes and top view of each of these (hkl) planes.

3. RESULTS AND DISCUSSION

The descending order of 43 average numbers of overlaps for G(001) plane on M(hkl), F(hkl), P(hkl), and C(hkl) planes show generally the highest values, i.e. the best structure compatibility, for M(hkl) planes (Figure 2). The highest and the second highest value is achieved for M(102)SiAlO1 (2482.006 ± 25.048) and M(010)SiAlO (2087.061 ± 32.127) planes, respectively. All numerical data are provided in Supplementary material [22]. In the group of phases formed from magnesium phyllosilicates, F(001)MgSiO (1984.681 ± 21.764) and P(100)O (1545.942 ± 19.360) planes on the 3rd and 8th position, respectively, exhibit the highest average number of overlaps (Figure 2). These values represent ~80% a ~62%, respectively, of the 1st value achieved for the M(102)SiAlO1 plane. The C(hkl) planes generally show the lowest average numbers of overlaps and from two-thirds are only found in the second half of all 43 values (Figure 2). The highest value (1428.375 ± 43.963) at the 14th position achieved for the C(100)SiO plane represents ~58% of the first value achieved for the M(102)SiAlO1 plane. Based on the average number of overlaps, the degree of structure compatibility of the studied phases with the G(001) plane can be expressed as follows: M > F > P > C.

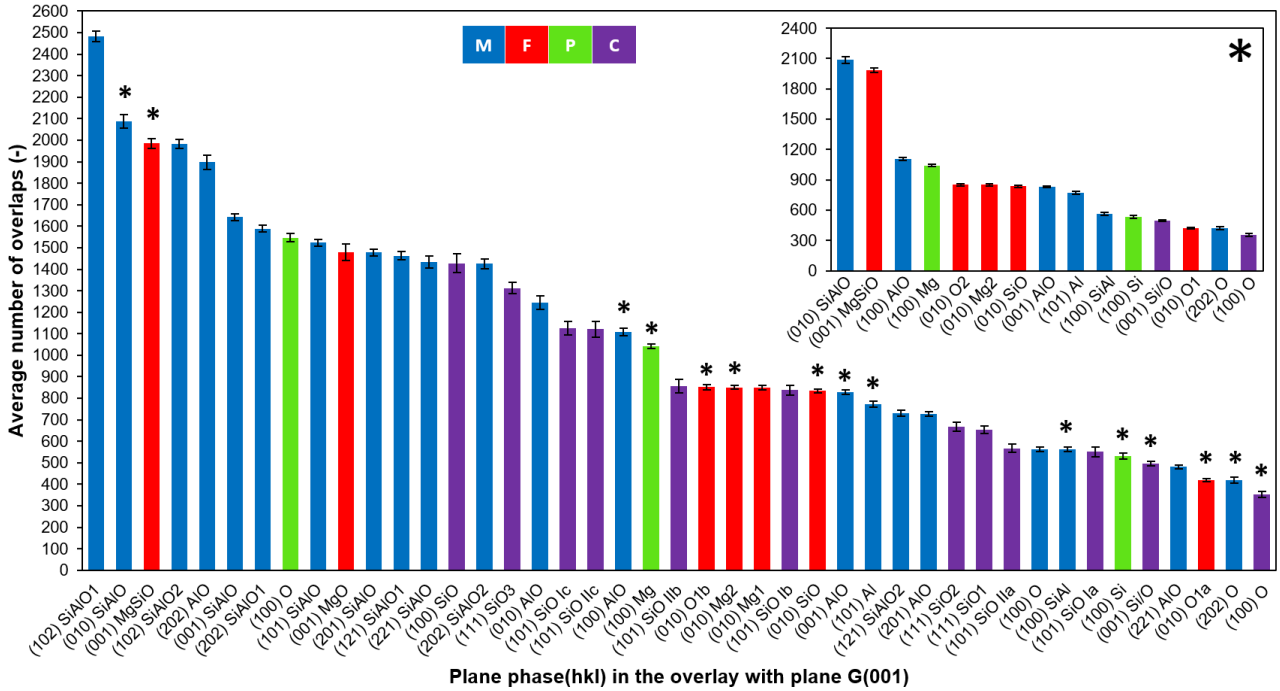

Figure 2 Descending order of the average number of overlaps for the G(001) plane on all M(hkl), F(hkl), P(hkl), and C(hkl) planes. Planar (hkl) planes formed by atoms lying in one geometric plane are marked with an asterisk. The inset compares the average numbers of overlaps for these planes only.

If only planar planes are considered, this order does not change (see the inset in **Figure 2**). The M phase still shows the highest average number of overlaps (2087.061 ± 32.127), although the average number of overlaps for the F(001)MgSiO plane begin to approach it much closer in this case (1984.681 ± 21.764) than when all (hkl) planes are compared regardless of planarity.

Figure 3 shows that the dependence of average numbers of overlaps is generally not directly proportional to the deviation from planarity. The reason for the higher values of the average number of overlaps is therefore not the increased density of atoms in non-planar (hkl) planes after the inclusion of slightly deviated atoms, but better structural compatibility based on a more similar arrangement of atoms in the G(001) plane and the given phase(hkl) planes (whether planar or not). All numerical data are provided in Supplementary material [22].

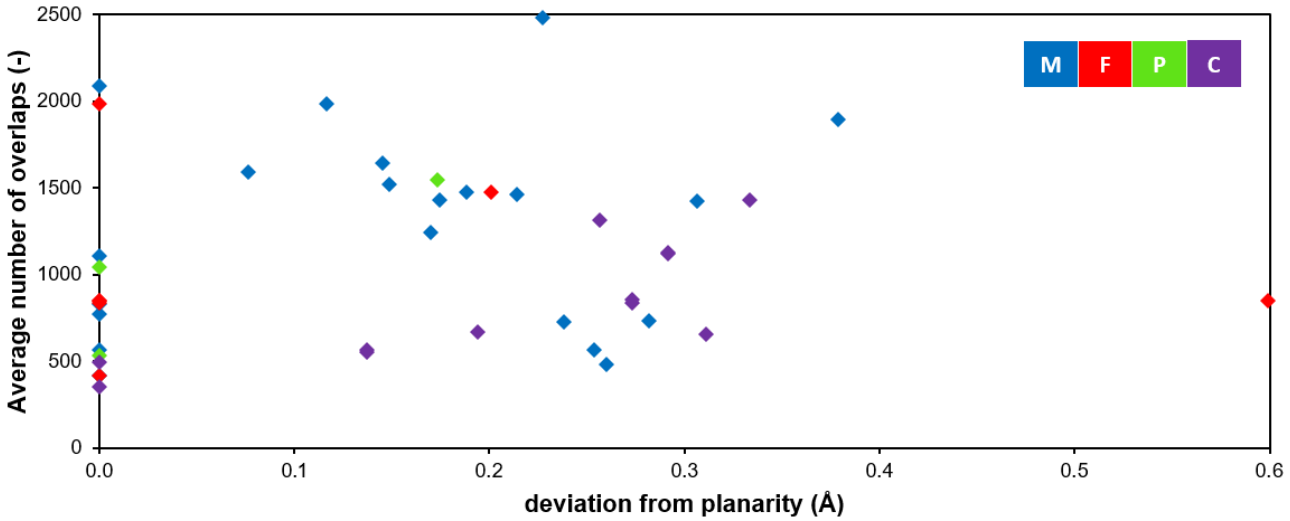

Figure 3 Dependence of the average numbers of overlaps on deviations from ideal planarity. For perfectly planar (hkl) planes, the deviation is zero.

In addition to the numerical values of the number of overlaps, the structure compatibility calculation also provides a visualization of these overlaps for each G(001) in-plane orientation on each phase(hkl) plane. Visualizations of the orientations leading to the highest number of overlaps for each of the M, F, P and C phases can be seen in **Figure 4**. For clarity, only smaller regions (50×50 Å) are shown. Full-size visualizations of the 100×100 Å areas are provided in the Supplementary material [22].

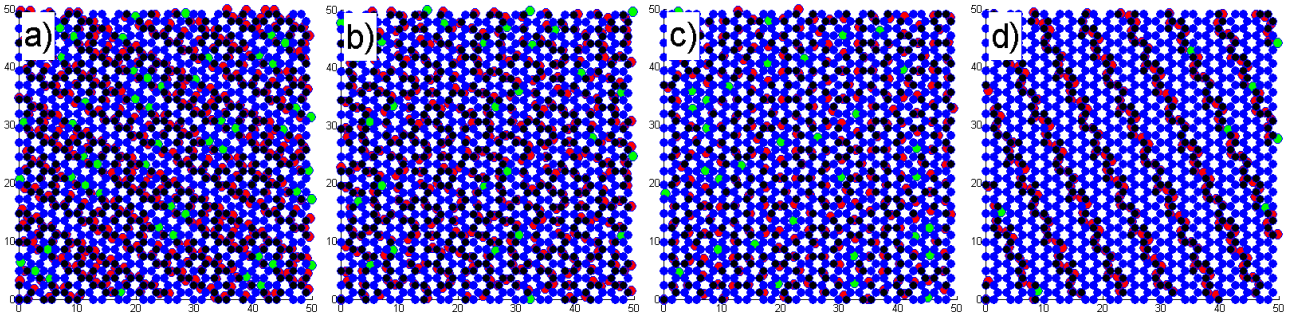

Figure 4 Visualization of the G(001) orientations leading to the highest number of overlaps on each of the phases: (a) M(102)SiAlO1, (b) F(001)MgSiO, (c) P(100)O, (d) C(100)SiO. Color legend: blue – non overlapping atoms in G(001) plane, black - overlapping atoms in G(001) plane, green – non overlapping atoms in phase(hkl) plane, red – overlapping atoms in phase(hkl) plane.

Distinct differences in the distribution of G(001) and phase(hkl) overlapping atoms are apparent. In the case of M(102)SiAlO1, a relatively regular pattern of overlaps can be observed, with the overlaps filling a significant

part of the area leaving only tiny regions (~ 5×3 Å) of incompatibility (**Figure 4a**). In the case of F(001)MgSiO and P(100)O, the overlaps form an irregular network of interconnected meshes, denser for F(001)MgSiO and sparser for P(100)O (compare **Figures 4b** and **4c)**. In the case of C(100)SiO, the overlaps form narrow parallel bands with "empty" regions approximately 5 Å wide (**Figure 4d**). An overview of the visualizations for the other phase(hkl) planes (see the Supplementary material [22]) shows that the least discontinuous distribution of overlaps is achieved for G(001) on the M(hkl) and F(hkl) planes.

4. CONCLUSION

The results achieved for the G(001) plane on the (hkl) planes of M, F, P and C phases formed by heat treatment of Al-rich and Mg-rich phyllosilicates revealed the best structure compatibility for G(001) and M(hkl). This confirms the empirical experience that nanocomposites containing graphitic carbon can be successfully prepared in situ by thermal treatment of organics with montmorillonite (Al-rich phyllosilicate), which is most often used for this purpose [1-5,8,10,11,13-15]. Relatively high numbers of overlaps found for some F(hkl) and P(hkl) planes suggests that Mg-rich phyllosilicates may also be suitable for this purpose. This is also supported by visualizations of the G(001) on those M, F, P, and C planes that lead to the maximum number of overlaps for each of the phases. The distribution of overlaps more or less over the entire area found for M, F, and P shows these planes as more suitable substrates for continuous growth of G(001) compared to the C plane. Future research will be focused on the correlation of obtained data with real samples prepared in situ by heat treatment of organics not only in the presence of phyllosilicates, but also in the presence of pure M, F, P, and C phases.

ACKNOWLEDGEMENTS

This work was supported by The Ministry of Education, Youth and Sports of the Czech Republic from the projects SGS (SP2024/041) and MATUR - Materials and Technologies for Sustainable Development (CZ.02.01.01/00/22_008/0004631).

REFERENCES

[1] SONOBE, N., KYOTANI, T., HISHIYAMA, Y., SHIRAISHI, M., TOMITA, A. Formation of highly oriented graphite from poly(acrylonitrile) prepared between the lamellae of montmorillonite. *J. Phys. Chem*. 1988, vol. 92, pp. 7029–7034. https://doi.org/10.1021/j100335a037

[2] SONOBE, N., KYOTANI, T., TOMITA, A. Carbonization of polyacrylonitrile in a two-dimensional space between montmorillonite lamellae. *Carbon*. 1988, vol. 26, pp. 573-578. https://doi.org/10.1016/0008-6223(88)90158-3

[3] KYOTANI, T., SONOBE, N., TOMITA, A. Formation of highly orientated graphite from polyacrylonitrile by using a two-dimensional space between montmorillonite lamellae. *Nature*. 1988, vol. 331, pp. 331-333. https://doi.org/10.1038/331331a0

[4] SONOBE, N., KYOTANI, T., TOMITA, A. Carbonization of polyfurfuryl alcohol and polyvinyl acetate between the lamellae of montmorillonite. *Carbon*. 1990, vol. 28, pp. 483-488. https://doi.org/10.1016/0008-6223(90)90042-W

[5] WINANS, R.E., CARRADO, K.A. Novel forms of carbon as potential anodes for lithium batteries. *Journal of Power Sources*. 1995, vol. 54, pp. 11-15. https://doi.org/10.1016/0378-7753(94)02032-X

[6] SANDÍ, G., WINANS, R.E., SEIFERT, S., CARRADO, K.A. In situ SAXS studies of the structural changes of sepiolite clay and sepiolite-carbon composites with temperature. *Chemistry of Materials*. 2002, vol. 14, pp. 739-742. https://doi.org/10.1021/cm010627w

[7] FERNÁNDEZ-SAAVEDRA, R., ARANDA, P., RUIZ-HITZKY, E. Templated synthesis of carbon nanofibers from polyacrylonitrile using sepiolite. *Advanced Functional Materials.* 2004, vol. 14, pp. 77-82. https://doi.org/10.1002/adfm.200305514

[8] RUIZ-HITZKY, E., DARDER, M., FERNANDES, F.M., ZATILE, E., PALOMARES, F.J., ARANDA, P. Supported graphene from natural resources: easy preparation and applications. *Advanced Materials.* 2011, vol. 23, pp. 5250-5255. https://doi.org/10.1002/adma.201101988

[9] ANDRADE, P.F., AZEVEDO, T.F., GIMENEZ, I.F., SOUZA FILHO, A.G., BARRETO, L.S. Conductive carbon–clay nanocomposites from petroleum oily sludge. *Journal of Hazardous Materials.* 2009, vol. 167, pp. 879-884. https://doi.org/10.1016/j.jhazmat.2009.01.070

[10] DING, W., WEI, Z., CHEN, S., QI, X., YANG, T., HU, J., WANG, D., WAN, L.-J., ALVI, S.F., LI, L. Space-confinement-induced synthesis of pyridinic- and pyrrolic-nitrogen-doped graphene for the catalysis of oxygen reduction. *Angewandte Chemie International Edition*. 2013, vol. 52, pp. 11755-11759. https://doi.org/10.1002/anie.201303924

[11] RUIZ-GARCIA, C., PÉREZ-CARVAJAL, J., BERENGUER-MURCIA A., DARDER, M., ARANDA, P., CAZORLA-AMORÓS, D., RUIZ-HITZKY, E. Clay-supported graphene materials: application to hydrogen storage. *Physical Chemistry Chemical Physics*. 2013, vol. 15, pp. 18635-18641. https://doi.org/10.1039/c3cp53258e

[12] ZHANG, Y., OUYANG, J., YANG, H. Metal oxide nanoparticles deposited onto carbon-coated halloysite nanotubes. *Applied Clay Science*. 2014, vol. 95, pp. 252-259. http://dx.doi.org/10.1016/j.clay.2014.04.019

[13] MICÓ VICENT, B., LÓPEZ, M., BELLO, A., MARTÍNEZ, N., MARTÍNEZ VERDÚ, F., Optimum multilayer-graphene-montmorillonite composites from sugar for thermosolar coatings formulations. *Journal of Solar Energy Engineering*. 2017, vol. 139, pp. 1-7. https://doi.org/10.1115/1.4035757

[14] WANG, J., XU, Y., DING, B., CHANG, Z., ZHANG, X., YAMAUCHI, Y., WU, K.C.W. Confined self-assembly in two-dimensional interlayer space: Monolayered mesoporous carbon nanosheets with in-plane orderly arranged mesopores and a highly graphitized framework. *Angewandte Chemie International Edition*. 2018, vol. 57, pp. 2894-2898. https://doi.org/10.1002/anie.201712959

[15] TOKARSKÝ, J., MAMULOVÁ KUTLÁKOVÁ, K., PEIKERTOVÁ, P., ŘEHÁČKOVÁ, L., KORMUNDA, M., MATĚJKOVÁ, P., ŠTUDENTOVÁ, S., KULHÁNKOVÁ, L. Polypyrrole/montmorillonite and polypyrrole/ghassoul intercalates as a source of graphite and multi-layer graphene: preparation of nanocomposites exhibiting strongly anisotropic electrical conductivity. *Materials Research Bulletin.* 2021, vol. 142, pp. 111429. https://doi.org/10.1016/j.materresbull.2021.111429

[16] YALCINKAYA, E., BASKAN-BAYRAK, H., OKAN B.S. Growing of 2D/3D graphene structures on natural substrates from aromatic plastic wastes by scalable thermal-based upcycling process with a comparative CO_2 footprint analysis. *Sustainable Materials and Technologies.* 2023, vol. 37, pp. e00687. https://doi.org/10.1016/j.susmat.2023.e00687

[17] BARRA, A., LAZAR, O., MIHAI, G., BRATU, C., RUIZ-GARCIA C., DARDER, M., ARANDA, P., ENACHESCU, M., NUNES, C., FERREIRA, P., RUIZ-HITZKY E. Graphene-like materials supported on sepiolite clay synthesized at relatively low temperature. *Carbon*. 2024, vol. 218, pp. 118767. https://doi.org/10.1016/j.carbon.2023.118767

[18] TOKARSKÝ, J., MOLEK, J. Overlap and rotate - a simple method for predicting out-of-plane and in-plane orientations of heteroepitaxial thin films. *Surfaces and Interfaces*. 2024, vol. 46, pp. 104129. https://doi.org/10.1016/j.surfin.2024.104129

[19] CORDERO, B., GÓMEZ, V., PLATERO-PRATS, A.E., REVÉS, M., ECHEVERRÍA, J., CREMADES, E., BARRAGÁN, F., ALVAREZ, S. Covalent radii revisited. *Dalton Transactions*. 2008, vol. 21, pp. 2832-2838.

[20] WYCKOFF, R.W.G., *Crystal Structures, second ed., Volume 1*, New York: John Wiley & Sons, Inc., 1963.

[21] WYCKOFF, R.W.G., *Crystal Structures, second ed., Volume 4, Miscellaneous Inorganic Compounds, Silicates, and Basic Structural Information*, New York: John Wiley & Sons, Inc., 1968.

[22] Data collection. *Dataset for Structure compatibility of graphite and phases formed from aluminum or magnesium phyllosilicates*. [online]. 2024. [viewed: 2024-09-27]. Available from: https://doi.org/ 10.5281/zenodo.11574074